On the use of Gibbs Sampling for Inter-Cell Interference Mitigation under Partial Frequency Reuse Schemes

K. Koutlia, J. Pérez-Romero, R. Agustí
Dept. of Signal Theory and Communications (TSC)
Universitat Politècnica de Catalunya (UPC)
Barcelona, Spain
Email: {katkoutlia, jorperez, ramon}@tsc.upc.edu

M. Žiak
Department of Telecommunications and Multimedia
University of Žilina
Žilina, Slovakia
Email: {ziak.mato@gmail.com}

***Abstract*—Fourth Generation (4G) cellular networks present a number of improvements in the overall network performance. However, and despite the advanced technologies that are being employed, Inter Cell Interference (ICI) remains a constraining factor. ICI Coordination techniques target the minimization of ICI and have gained ground in the literature. The introduction of dynamicity in these schemes results in even better bandwidth utilization and enhances the overall performance. In this work, we propose a distributed algorithm that performs dynamic channel allocation to mitigate the ICI in cellular scenarios applying Partial Frequency Reuse (PFR). In particular, the algorithm is based on a Gibbs Sampler mechanism that allows achieving an optimized performance. Simulation results have shown that the proposed solution reduces the network interference up to 13 dB with respect to classical PFR. In addition, benefits have also been observed in the user capacity, where our scheme achieves improvements of up to 43% in terms of average user capacity and up to 17% for the users located at the cell edge.**

Keywords—Dynamic Frequency Allocation; Partial Frequency Reuse; Gibbs Sampler

I. INTRODUCTION

The new era of mobile communications is dictated by the usage of smartphones, tablets and laptops and their demand for high data rate applications and seamless connections. The introduction of the fourth generation (4G) cellular systems has been a crucial point in the history of mobile communications evolution, targeting improved coverage, enhanced capacity and robust, high speed data transfer. Third Generation Partnership Project (3GPP) has adopted Orthogonal Frequency Division Multiple Access (OFDMA) as radio access technology in 4G networks, resulting in better spectral efficiency and in the reduction of the Intra-Cell Interference, due to the orthogonality of the users. However, despite its significant contribution to the overall network performance, Inter-Cell Interference (ICI) can degrade the achievable capacity. Especially for the edge users, which are located close to the cell borders, ICI becomes a constraining factor resulting in a considerable capacity reduction for these users.

In order to cope with the above mentioned problem, 4G systems make use of ICI coordination (ICIC) techniques. These schemes allow the allocation of the available resources to the edge users with higher reuse factors, mitigating in this way the network interference [1]. ICIC techniques usually follow the general concept of Fractional Frequency Reuse (FFR) [2], where the cell is divided in two areas, the inner and the outer, and the same strategy is applied to the available bandwidth.

Different schemes have been proposed for FFR, such as Soft Frequency Reuse (SFR) [3] and Partial Frequency Reuse (PFR) [4][5]. This work focuses on the PFR scheme that splits the cell in two regions, the inner and the outer, as illustrated in Figure 1. In the same way, the bandwidth is divided into the inner band, assigned with a reuse-1 factor (Full Reuse) so that it is common to all the cells, and the outer band, which is assigned with a higher reuse factor (Partial Reuse), e.g., reuse-3, as it can be seen in the right part of Figure 1, where the frequency bands assigned to each inner/outer cell are presented. In addition, PFR allows the possibility for different powers to be used for the downlink (DL) transmissions in the inner/outer parts of the cell.

However, despite of the advantages of the classical PFR schemes, the allocation of the resources follows a static principle. As a result, since the network traffic conditions vary over time, a static allocation will not be able to adapt to these changes [6]. Moreover, these schemes may not be optimal in irregular deployments. As such, research has been focused on the optimization of the ICIC schemes though the introduction of dynamicity. A Dynamic Fractional Frequency Reuse scheme has been presented in [7] making use of a graph-based framework to re-allocate resources depending on cell load variations. In [8], the authors presented a Dynamic Frequency Reuse scheme that mainly deals with uneven traffic loads. Two algorithms are used, one for resource allocation and another one for power control, which significantly improved the network capacity and the energy efficiency. In [9], an adaptive PFR scheme has been developed based on an off-line genetic algorithm enhancing the performance in terms of edge user throughput. Recently the FFR concept has also been proposed for interference management in heterogeneous networks involving both macro and femtocells as for example in [10].

Under the above presented framework, in this work we propose a novel dynamic allocation scheme based on the Gibbs Sampler [11][12] concept as optimization tool. The

 ISBN: 978-1-61208-313-1

proposed solution is applied in tri-sectorial PFR deployments targeting the minimization of the downlink ICI. The rationale behind this selection is that this mechanism accomplishes such an interference minimization in a natural way and it is an efficient tool for distributed optimization. In particular, this paper investigates how to optimally assign a set of frequencies in the inner and the outer parts of the different cells in the scenario. The proposed mechanism is suitable for 4G systems with special focus on 3GPP LTE since the partitioning of the available bandwidth in sub-bands and the X2 interface used for coordination purposes constitute it an ideal candidate.

Gibbs sampler-based algorithms for optimization purposes have been widely used in the literature under a variety of situations. Two fully distributed algorithms that follow the concept of Gibbs Sampler have been used in [13] in order to perform channel selection and user association in unmanaged WiFi networks. In [14], the authors have adopted this methodology to improve the performance of homogeneous cellular networks. The optimization targets the power control and the user association. Finally, in [15] a Gibbs sampler-based mechanism has been applied to perform joint optimization in heterogeneous networks.

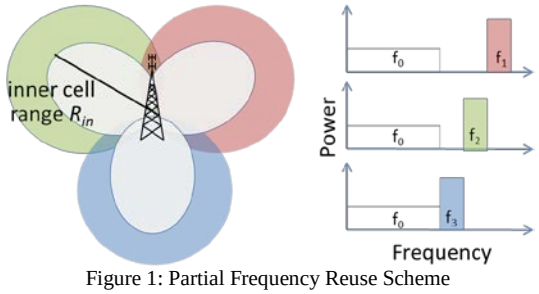

Figure 1: Partial Frequency Reuse Scheme

The rest of the paper is organized as follows. In Section II, a description of the system model and the definition of the notation used throughout the text are given. The optimization model and the algorithm formulation are presented in Section III. In Section IV, the simulation model along with the evaluation of the algorithm performance are presented. Finally, important conclusions and the future work are given in Section V.

II. System Model

The system model of this work consists of a cellular network where N Base Stations are spatially divided in three sectors (cells) with the use of directional antennas, resulting in a set of cells X.

Users are randomly distributed in the scenario and each user is associated with the cell with which experiences the minimum Path Loss described by the following equation:

$$L_{u,x}(dB) = l_A + l_B \log d_{u,x}(km) - B(\phi_{u,x}, \theta_{u,x}) + S_{u,x} \quad (1)$$

where $d_{u,x}$ is the distance between user u and cell x, l_A and l_B are parameters of the propagation model that depend on the considered environment, $S_{u,x}$ is a Gaussian random variable representing the Log-Normal Shadowing between user u and cell x and $B(\phi_{u,x}, \theta_{u,x}) = B_H(\phi_{u,x}) + B_V(\theta_{u,x})$ is the antenna pattern decomposed into the horizontal $B_H(\phi_{u,x})$ and the vertical $B_V(\theta_{u,x})$ patterns calculated using the following formulas in dB [16]:

$$B_H(\phi_{u,x}) = -min\left(B_o, 12 \cdot \left(\frac{\phi_{u,x} - \Phi}{\Delta_\phi}\right)^2\right) \quad (2)$$

$$B_V(\theta_{u,x}) = -min\left(B_o, 12 \cdot \left(\frac{\theta_{u,x} - \Theta}{\Delta_\theta}\right)^2\right) \quad (3)$$

where $\phi_{u,x}$ and $\theta_{u,x}$ are the azimuth and elevation angles, respectively, between user u and cell x. Moreover, Φ and Θ are the azimuth and downtilt orientations of the antennas, respectively, Δ_ϕ is the horizontal antenna beam width, Δ_θ is the vertical antenna beam width and B_o is the backward attenuation.

The set of users that is associated with cell $x \in X$ is denoted as U_x. Each user is classified as inner or outer according to a Path Loss Threshold L_{th} that is related to the inner cell range R_{in} as follows:

$$L_{th}(dB) = l_A + l_B \log R_{in}(km) \quad (4)$$

Specifically, a user u associated to cell x belongs to the inner part of the cell if its path loss $L_{u,x}$ is lower than L_{th}. Otherwise, it belongs to the outer part of the cell. Note that L_{th} is the average path loss that it would be observed by a user located at distance R_{in} in the direction of maximum radiated power by the antenna $\phi_{u,x} = \Phi$ and $\theta_{u,x} = \Theta$. As such, the set of users is further split into the inner set $U_{x,in}$ and the outer set $U_{x,out}$. Since the calculation of each users Path Loss includes also the Shadowing, the consideration of a user being inner or outer is not only related to its distance from the base station, but it also accounts for the randomness in the propagation that is inherent to practical wireless scenarios.

Let us consider a set of C frequency channels or sub-bands to be shared among the set of X cells. The bandwidth of each channel $c \in C$ is B_c. For simplicity reasons we assume that each cell can be assigned only one channel for the inner and another one for the outer part; however this work can be easily extended to assign a group of frequencies to each cell. Then, at a given point of time each cell x is characterized by its state $c_x = (c_{x,in}, c_{x,out})$ that is given by the channel $c_{x,in} \in C$ assigned to the inner part and the channel $c_{x,out} \in C$ assigned to the outer part. In order to avoid that the same channel is shared by inner and outer users the allocation will ensure that different channels are assigned to the inner and the outer parts, that is $c_{x,in} \neq c_{x,out}$.

Moreover, we consider that the transmit power of a given cell x in channel c is:

$$P_{x,c} = \begin{cases} P_{x,out} & \text{if } c_{x,out} = c \\ P_{x,in} & \text{if } c_{x,in} = c \\ 0 & otherwise \end{cases} \quad (5)$$

where $P_{x,in}$ and $P_{x,out}$ are the transmit power (in W) of cell x for the inner and the outer parts, respectively.

Based on the above, the Signal to Interference and Noise Ratio (SINR) for an inner user $u_{x,in} \in U_{x,in}$ of cell x is then expressed by the following equation:

$$SINR_{u_{x,in}} = \frac{\frac{P_{x,c_{x,in}}}{L_{u_{x,in},x}}}{P_N + \sum_{k \neq x} \frac{P_{k,c_{x,in}}}{L_{u_{x,in},k}}} \quad (6)$$

where P_N is the noise power (in W) and $k \in X$ denotes the interfering cells. $L_{u_x,x}$ and $L_{u_x,k}$ respectively denote the Path Loss (in linear units) of user u_x with its serving cell x and with the interfering cell k.

We assume that the bandwidth of one channel in the inner/outer part is equally shared between all users of the inner/outer part. This would correspond to, e.g., a round robin scheduling. In that case, the total capacity (b/s) seen by an inner user of cell x (using Shannon capacity) is:

$$C_{u_{x,in}} = \frac{B_{c_{x,in}}}{|U_{x,in}|} \log_2 \left(1 + SINR_{u_{x,in}}\right) \quad (7)$$

where $|.|$ denotes cardinality. Note that the same expressions (6) and (7) apply for the outer users by simply replacing the *in* sub-index by *out*.

Then, the average capacity per user in the scenario is:

$$C_{user,avg} = \frac{\sum_x \sum_{u_{x,in}} C_{u_{x,in}} + \sum_x \sum_{u_{x,out}} C_{u_{x,out}}}{\sum_x \left(|U_{x,in}| + |U_{x,out}|\right)} \quad (8)$$

The target of this work is to find the optimal allocation of frequencies to the inner and the outer parts of the cells (i.e. the optimal cell states c_x) that results in the minimization of the network inter-cell interference and thus, it enhances the capacity. For this purpose a Gibbs sampler-based methodology is proposed. In the following Section, a thorough description of the optimization model is given.

III. GIBBS SAMPLER FOR CHANNEL ALLOCATION

The Gibbs Sampler uses the notion of *energy function* which is the optimization target and thus it should be defined in accordance with each specific problem [12]. Therefore, the following sub-sections present the formulation of the energy function considered in this paper for minimizing the ICI in accordance with the system model defined in previous section, and the distributed Gibbs-sampler based algorithm to achieve the minimization.

A. Optimization Model

The target of the proposed optimization approach is to find the states c_x (i.e. the channel allocation) for each cell that minimize the overall inter-cell interference. For that purpose, we define the *global energy* to be minimized as the total interference of the network which will be the sum of the total noise and the interference measured by all the cells:

$$\varepsilon = \sum_x \left[P_N + \frac{1}{|U_{x,in}|} \sum_{u_{x,in}} \sum_{k \neq x} \frac{P_{k,c_{x,in}}}{L_{u_{x,in},k}} + \frac{1}{|U_{x,out}|} \sum_{u_{x,out}} \sum_{k \neq x} \frac{P_{k,c_{x,out}}}{L_{u_{x,out},k}} \right] \quad (9)$$

Note that in the above expression we consider for each cell the average interference seen by its served users. Then, the *energy function* can be rewritten as:

$$\varepsilon = \sum_x P_N + \sum_{(x,k)} \left(f(k,x) + f(x,k) \right) \quad (10)$$

where $f(k,x)$ is the interference generated by cell k to cell x:

$$f(k,x) = \frac{1}{|U_{x,in}|} \sum_{u_{x,in}} \frac{P_{k,c_{x,in}}}{L_{u_{x,in},k}} + \frac{1}{|U_{x,out}|} \sum_{u_{x,out}} \frac{P_{k,c_{x,out}}}{L_{u_{x,out},k}} \quad (11)$$

As such, the *energy function* derives from the following *potential function V*(ν):

$$\varepsilon = \sum \left\{ V(\nu) \middle| \nu \subseteq X \right\} \quad (12)$$

where ν represents any possible subset of cells that can be formed with the elements of X and $V(\nu)$ is given by

$$V(\nu) = \begin{cases} P_N & \text{if} \quad \nu = \{x\} \\ f(k,x) + f(x,k) & \text{if} \quad \nu = \{x,k\} \\ 0 & \text{if} \quad |\nu| \geq 3 \end{cases} \quad (13)$$

A *global energy* which derives from the *potential function* (13) can be optimized using Gibbs with the following *local energy* for each cell x [11][15]:

$$\varepsilon_x = \sum \left\{ V(\nu) \middle| x \in \nu, \nu \subseteq X \right\} = P_N + \sum_{k \neq x} \left(f(k,x) + f(x,k) \right) \quad (14)$$

The Gibbs sampler will compute the *local energy* for each possible state of cell x, $c_x = (c_{x,in}, c_{x,out})$, as follows:

$$\varepsilon_x (c_{x,in}, c_{x,out}) = P_N + \sum_{k \neq x} \left(\frac{1}{|U_{x,in}|} \sum_{u_{x,in}} \frac{P_{k,c_{x,in}}}{L_{u_{x,in},k}} + \frac{1}{|U_{x,out}|} \sum_{u_{x,out}} \frac{P_{k,c_{x,out}}}{L_{u_{x,out},k}} \right) + \sum_{k \neq x} \left(\frac{1}{|U_{k,in}|} \sum_{u_{k,in}} \frac{P_{x,c_{k,in}}}{L_{u_{k,in},x}} + \frac{1}{|U_{k,out}|} \sum_{u_{k,out}} \frac{P_{x,c_{k,out}}}{L_{u_{k,out},x}} \right) \quad (15)$$

The *local energy* function actually includes the measurement of the interference that users of cell x will experience from the other cells if cell x state is c_x (second term of the equation), as well as the interference that cell x will cause to the neighboring cells (third term of the equation).

B. Algorithm

The minimization of the *energy function* given by (9) is achieved by means of the execution of the procedure indicated in the algorithm presented in Figure 2 at each cell.

Assuming that the system starting time is t=0, each cell is assigned with an exponentially distributed timer with mean t_a. When a cell's timer expires, the algorithm is executed and the state c_x selection (i.e. the set of channels $(c_{x,in}, c_{x,out})$) is carried out by sampling a random variable λ using the probability distribution of (16). The latter represents the probability of selecting state c_x among the set of all possible states denoted as C_S. The set C_S includes all the combinations $(c_{x,in}, c_{x,out})$ composed by $c_{x,in} \in C$ and $c_{x,out} \in C$ with $c_{x,in} \neq c_{x,out}$.

$$\pi(c_x) = \frac{e^{\left(-\varepsilon_x(c_{x,in},c_{x,out})/T\right)}}{\sum_{c' \in C_S} e^{\left(-\varepsilon_x(c'_{x,in},c'_{x,out})/T\right)}} \quad (16)$$

where T is the *temperature* parameter and is calculated as:

$$T = \frac{T_0}{\log_2(2+t)} \quad (17)$$

In this formula T_0 is a constant and t is the age variable representing the time passed since t=0.

1: **if** *cell x timer (T_x) expires at time t*
2: *calculate the temperature parameter T* (17)
3: **for** *each state $c_x \in C_S$*
4: *calculate the Local Energy* $\varepsilon_x(c_{x,in}, c_{x,out})$ (15)
5: *calculate the Selection Probability* $\pi(c_x)$ (16)
6: **end for**
7: *sample a random variable λ with law $\pi(c_x)$*
8: *assign channels $(c_{x,in}, c_{x,out})$ according to the outcome of λ*
9: *sample an exponential random variable μ with mean t_a*
10: *assign a new timer (T_x=t+μ)*
11: **end if**

Figure 2: Algorithm of the Gibbs Sampler Procedure

After the state selection is performed for a given cell, a new timer is generated to schedule the subsequent execution of the algorithm. The probability distribution described above favors the lower energy states and with $T \rightarrow 0$ it will converge to a steady state that minimizes the *global interference*.

IV. Simulation Results

The performance of the proposed algorithm has been evaluated by means of system level simulations. In this section we present the simulation model and the parameters used, as well as the most important results.

A. Simulation scenario and parameters

The cellular network deployment consists of 4 tri-sectorial base stations, thus having a total of 12 cells, as depicted in Figure 3. The set of channels that can be assigned are $C = \{f_0, f_1, f_2, f_3\}$ with the restriction that $c_{out} \neq c_{in}$. As such, there is a total of 12 possible states to be selected for each cell. Figure 3 depicts the classical PFR scheme that is used as reference for the comparison and evaluation of the results. Moreover, for the Gibbs sampler-based algorithm it is assumed that the initial allocation considered in the beginning of each simulation is also the one shown in Figure 3.

Each cell serves 10 users uniformly distributed in a circular area with range R=1 *km*. The total simulation time is $12000 \cdot t_a$ and the simulation step is $t_a/24$. T_0 is set to 0.7 and the energy values in (15) are given in dBW. Simulations are performed for different values of the inner cell range R_{in}.

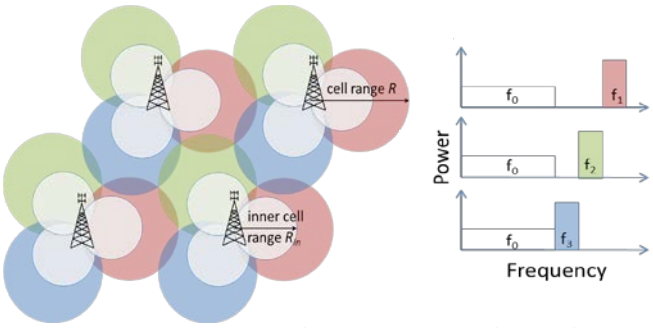

Figure 3: System Topology and frequency assignment for the reference case

The outer transmit power ($P_{x,out}$) is kept constant to 43 dBm in all the simulations, while the inner transmit power ($P_{x,in}$) is set according to the inner cell range (equivalently L_{th}) as follows:

$$P_{x,in}(dBm) = P_{x,out}(dBm) - l_A - l_B \log R(km) + L_{th} \quad (18)$$

The rationality of this expression is to have the same average received power level for an outer user located at a distance equal to the cell range R and for an inner user located at a distance equal to the inner cell range R_{in}.

The rest of simulation parameters are indicated in Table I.

TABLE I. Simulation Parameters

Simulation	Parameters
Antenna Pattern	Δ_ϕ=70º, Δ_θ=10º, B_o=20 dB, Φ=120º, Θ=0º
Shadowing Std. Deviation	10 dB
Path Loss Parameters	l_A= 128.1 dB , l_B= 37.6
Bandwidth per channel B_c	5MHz
Noise Power P_N	-100 dBm

B. Numerical Results

We evaluate our scenario under two different criteria. In the first part, an analysis of the performance of the algorithm is given according to the energy reduction (interference minimization) it provides. Similarly, in the second part, we analyze the effect of the proposed algorithm to the network and edge user capacity. Additional information will be presented related to the performance of the algorithm in terms of convergence and feasibility for real time execution.

It has to be noted that for each inner cell range the result is the average of 500 experiments with different random user

 ISBN: 978-1-61208-313-1

distributions. For the comparison of the results we use as reference the PFR scheme presented in Figure 2.

1. *Global Energy Reduction:* Figure 4 shows the comparison of the global energy (in dBW) between the proposed solution and the reference scheme of Figure 3, where the Gibbs Sampler is not applied.

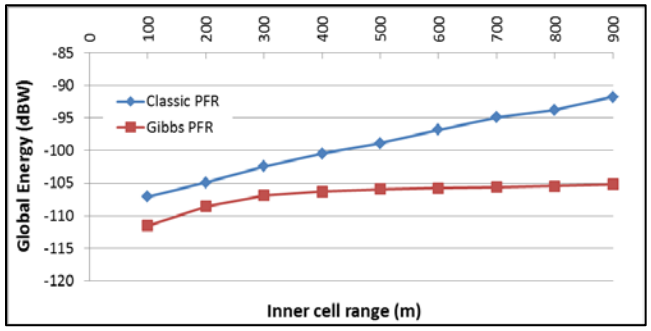

Figure 4: Global Energy

By studying the behavior of the energy, one can notice that there is a significant benefit from the execution of the algorithm, especially when considering inner cell ranges from 400 m and above. The highest gain of 13.43 dB is observed for the range of 900 m, while the average gain for all the inner cell ranges is 8.47 dB. If we focus on the reference scheme, it can be seen that the inner parts of all the cells of the network are assigned the same frequency (f_0). As such, the amount of the interference that these users experience, especially for high inner cell ranges, is quite high. This justifies the increasing behavior of the global energy when increasing the inner cell range. However, after the execution of the algorithm, the inner parts are assigned different frequencies resulting in this way in a significant interference reduction. It can also be observed that the global energy level for inner cell ranges above approximately 500m is kept at a very similar level.

2. *Capacity Improvement:* The benefits of the proposed PFR algorithm in ICI reduction are also reflected in terms of capacity improvement. This can be observed in Figure 5 that shows the average capacity for the users located at the cell edge, which are those more sensitive to ICI. For this computation, users are considered to be at the cell edge if they are located at a distance above 0.9*R* (note that edge users can be outer or inner users depending on the considered inner cell range in each simulation and also depending on shadowing conditions). As it is reflected from the figure, the edge user capacity is significantly improved compared to the classic PFR scheme. The maximum gain is observed for the inner cell range of 900 m, which reaches a capacity increase of 17%, and the average gain for all the inner cell ranges is 11.64%.

Furthermore, Figure 6 shows the comparison in terms of average capacity per user taking into consideration all the users in the cell. Similarly to the edge users, the highest gain is observed for the inner cell range of 900 m and reaches the value of 42.67%. The average gain in this case is 22.53%.

It can also be observed in Figure 5 and Figure 6 that, while the maximum average user capacity occurs for an inner cell range of 400m, when considering cell edge users, the maximum occurs for larger values. This is due to the fact that, for large inner cell ranges, in addition to the ICI reduction brought by the algorithm, the edge users share the available capacity with fewer users, since the outer area is reduced. Then, the optimal setting of the inner cell range would result from the trade-off between average and cell-edge capacity, in accordance with network operator policies.

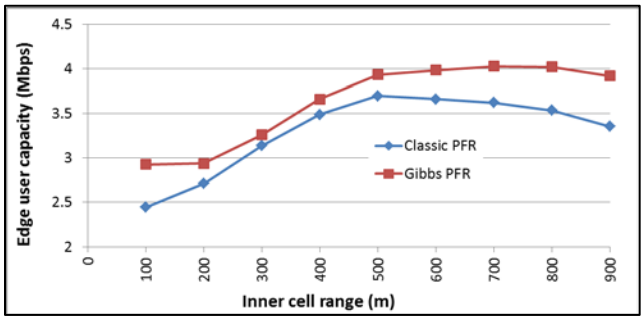

Figure 5: Average Edge User Capacity

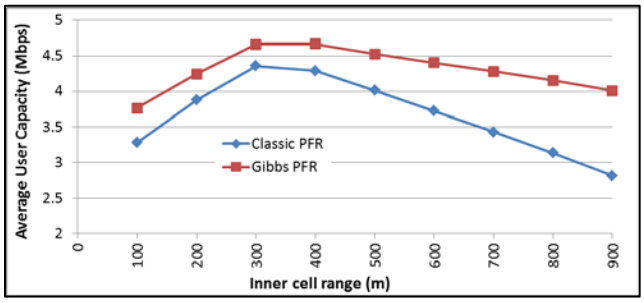

Figure 6: Average User Capacity

3. *Convergence of the algorithm:* In order to analyze the convergence of the algorithm, in this work we consider that the algorithm is executed either until a convergence criterion or the total simulation time ($12000 \cdot t_a$) is reached. The convergence criterion in this paper is that all the cells have reached a selection probability according to (16) above 0.99 for one of the possible states (then this state determines the assigned frequencies).

In Figure 7, we present the average number of the experiments that have met the convergence criterion of this paper as a result from the execution of 500 experiments for each inner cell range. It can be noticed that above the 400 m a significant amount of experiments has met the criterion. For smaller inner ranges however, it can be seen that this number very small. This was expected, since for these ranges the number of inner users is very small and in some cases there are cells with no inner users. Correspondingly, there exist actually multiple solutions that are optimal (e.g., for a cell without inner users the allocation of the inner channel does not affect the received inter-cell interference). In these situations, it has been observed that the algorithm does not converge towards a high probability for a given state but it keeps similar probability levels for all the optimum states. A similar effect is also observed for the larger cell ranges in the

 ISBN: 978-1-61208-313-1

particular cases that the convergence criterion is not met. The algorithm keeps similar probabilities for some states that exhibit the lowest energy. This behavior reflects the good operation of the algorithm.

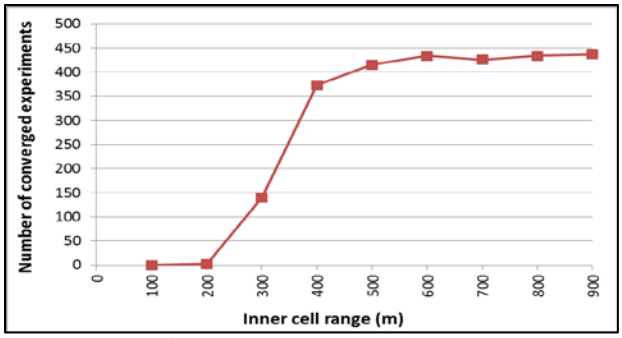

Figure 7: Number of experiments that have met the convergence criterion considered in this paper

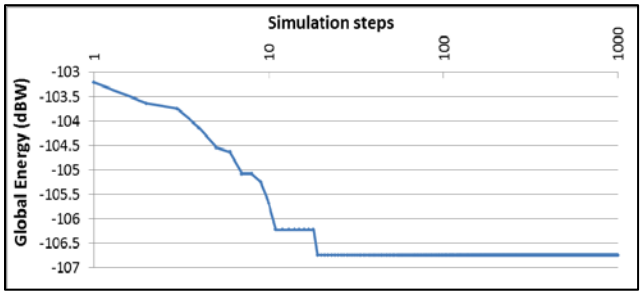

Figure 8: Global Energy Evolution

Another important aspect to evaluate the performance of the algorithm is the required number of executions in order to reach convergence. In that respect, Figure 8 presents the time evolution of the global energy of a random experiment, until the convergence criterion was met. In this particular experiment the algorithm reached convergence after 19 executions. Moreover, as it can be seen from the figure, the reduction of the energy is carried out continuously during the simulation time, suggesting this way the possibility of the online implementation of the algorithm.

V. CONCLUSIONS AND FUTURE WORK

In this paper we have proposed a new distributed algorithm based on Gibbs sampling that performs dynamic channel allocation in a PFR cellular deployment. Through simulations it has been proved that the proposed solution outperforms the classical PFR scheme in terms of interference and capacity. Results have shown the reduction of the network interference of up to 13 dB. Moreover, the proposed scheme provides a significant capacity improvement for the edge users with gains up to 17%, and up to 42.67% when considering the average capacity of all the users in the cell.

Further details about the specific implementation are envisaged as part of our future work, including the measurements involved and the information exchange between cells. Moreover, future work is envisaged to include the capacity optimization explicitly in the formulation, as well as the extension of the algorithm to adjust the transmit power of the cell. Finally, heterogeneous networks will be investigated, including macro and small cells.

ACKNOWLEDGMENT

This work has been supported by FP7 NEWCOM# project (grant number 318306) and by the Spanish Research Council and FEDER funds under ARCO grant (ref. TEC2010-15198).

REFERENCES

[1] G. Boudreau, J. Panicker, N. Guo, R Chang, N. Wang, and S. Vrzic, “Interference coordination and Cancellation in 4G Networks”, IEEE Communications Magazine, vol. 47, no. 4, April 2009, pp. 74-81.

[2] K. Begain, G.I. Rozsa, A. Pfening, and M. Telek, “Performance analysis of GSM networks with intelligent underlay-overlay”, ISCC , July 2002, pp. 135-141.

[3] 3GPP R1-050507 “Soft Frequency Reuse Scheme for UTRAN LTE”, 3GPP TSG RAN WG1 Meeting #41, May 2005.

[4] R1-050738, “Interference mitigation – Considerations and Results on Frequency Reuse”, RAN WG1#42, Aug./Sept. 2005.

[5] M. Sternad, T. Ottosson, A. Ahlen, and A. Svensson, “Attaining both coverage and high spectral efficiency with adaptive OFDM downlinks”, IEEE VTC, Oct. 2003, pp. 2486-2490.

[6] D. Lopez-Perez, A. Juttner, and J. Zhang, “Dynamic Frequency planning versus Frequency Reuse Schemes in OFDMA Networks”, IEEE VTC 69th, April 2009, pp.1-5.

[7] R. Chang, Z. Tao, J. Zhang, and C.-C. Jay Kuo, “Dynamic Fractional Frequency Reuse (D-FFR) for multicell OFDMA Networks using a graph framework”, Wirel. Commun. Mob. Comput., Jan. 2011, pp. 12-27.

[8] X. Shui, M. Zhao, P. Dong, and J. Kong, “A novel dynamic soft frequency reuse combined with power re-allocation in LTE uplinks”, WCSP, Oct. 2012, pp.1-6.

[9] G. Koudouridis, C. Qvarfordt, T. Cai, and J. Johansson, "Partial Frequency Allocation in Downlink OFDMA Based on Evolutionary Algorithms", IEEE VTC 72nd, Sep. 2010, pp.1-5.

[10] C. Kosta, A. Imran, A.U. Quddus, and R. Tafazolli, “Flexible Soft Frequency Reuse Schemes for Heterogeneous Networks (Macrocell and Femtocell)”, IEEE VTC 73rd, May 2011, pp.1-5.

[11] P. Bremaud, Markov Chains: Gibbs Field, Monte Carlo Simulation, and Queues, Springer Verlag, 1999.

[12] G. Winkler, “Image Analysis, Random Fields and Markov Chain Monte Carlo Methods: A Mathematical Introduction (Stochastic Modelling and Applied Probability)”, Springer-Verlag, New York, Inc., Secaucus, NJ, USA, 1995.

[13] B. Kauffman, F. Baccelli, A. Chaintreau, V. Mhatre, K. Papagiannaki, and C. Diot, “Measurement-based Self Organization of Interfering 802.11 Wireless Access Networks”, IEEE INFOCOM, May 2007, pp.1451–1459.

[14] C.Chen and F. Baccelli, “Self - Optimization in Mobile Cellular Networks: Power Control and User Association”, IEEE ICC, May 2010, pp. 1-6.

[15] C. S. Chen, F. Baccelli, and L. Roullet, "Joint Optimization of Radio Resources in Small and Macro Cell Networks," IEEE VTC, May 2011, pp.1-5.

[16] I. Viering M. Dottling, and A. Lobinger, “A mathematical perspective of self – optimizing wireless networks”, IEEE ICC Conference, 2009, pp. 1-6.

 ISBN: 978-1-61208-313-1